Available online at www.sciencedirect.com
SCIENCE DIRECT®
PERGAMON
Radiation Physics and Chemistry 68 (2003) 419–425
Radiation Physics and Chemistry
www.elsevier.com/locate/radphyschem

A multicell trap to confine large numbers of positrons

C.M. Surko[a,*], R.G. Greaves[b]

[a] Department of Physics, University of California, San Diego, 9500 Gilman Drive, La Jolla, CA 92093, USA
[b] First Point Scientific, Inc., Agoura Hills, CA 91301, USA

Abstract

The design of a multicell Penning–Malmberg trap capable of confining 10^{15} positrons is described. The motivation for choosing a multicell design is discussed, and key factors determining performance are identified. Specific issues for further research and development and possible extensions of this type of design are also discussed.

Keywords: Positrons; Traps; Single-component plasmas

1. Introduction

The ability to accumulate and store large numbers of positrons has the potential to open up a range of scientific and technological opportunities. For example, it would facilitate the study of Bose–Einstein condensation of positronium atoms (Platzman and Mills, 1994). It would also provide a means for studying electron–positron plasmas in parameter regimes of relevance in astrophysics (Greaves and Surko, 2002). Other potential uses include the creation of antihydrogen (Amoretti, 2002; Gabrielse, 2002), the production of intense pulses of positronium atoms (Surko et al., 1986), and the creation of a 511 keV gamma-ray laser (Mills, 2002). Furthermore, if positron storage could be achieved in portable devices, this could provide an attractive alternative to radioactive positron sources for laboratory positron beams (Greaves and Surko, 2002). These positron beams have a wide variety of applications in both the areas of basic physics research, such as atomic physics (Surko, 2001), as well as technological applications including materials analysis (Schultz and Lynn, 1988).

Various techniques have been considered for storing large numbers of positrons, including the use of electron–positron plasmas (Greaves and Surko, 2002), the creation of long-lived positronium (Ps) states in an electric field (Shertzer et al., 1998), and confinement in specially designed Penning–Malmberg traps (Greaves and Surko, 1997). Each of these methods has disadvantages of some kind. It appears, for example, that in the case of neutral electron–positron plasmas, outward plasma transport will be too rapid to make this a viable scheme for even short-term positron confinement (Greaves and Surko, 2002).

Advances in the accumulation of positrons in modified Penning traps (called Penning–Malmberg traps in the plasma community) (Greaves and Surko, 2002) make it timely to examine the physics issues and technological challenges of this technology as a candidate for accumulating large numbers of positrons. In particular, the recent demonstration of positron plasma compression by applying a rotating electric field (Hollmann et al., 2000; Greaves, 2001) provides a method for mitigating a major obstacle to using Penning traps for positron storage, namely the transport of the positron plasma across the confining magnetic field. In this paper, we discuss the design of a positron trap capable of storing 10^{15} positrons. This design is based on the present understanding of positron plasmas in Penning–Malmberg traps, including the confinement and cooling and the radial compression of these plasmas using a rotating electric field.

*Corresponding author. Tel.: +1-858-534-6880; fax: +1-858-534-0173.
E-mail address: csurko@ucsd.edu (C.M. Surko).

0969-806X/03/$ - see front matter
doi:10.1016/S0969-806X(03)00194-4

2. Brief overview of available tools

2.1. Penning–Malmberg traps

The Penning–Malmberg trap, illustrated in Fig. 1, consists of a set of cylindrical electrodes, biased in such a way as to create an axial confining electrostatic potential well, with radial confinement provided by a superimposed magnetic field. The central confining electrode is often divided axially into segments. It is also common to divide one or more of these segments azimuthally, as shown in Fig. 1. This segmentation permits various types of manipulations including plasma compression, heating, and excitation and sensing of plasma modes. Plasma properties can be diagnosed by releasing the plasma from the trap and collecting it on an electrode, which may be radially segmented to obtain radial profiles. Alternatively, as shown in Fig. 1, the plasma can be dumped onto a phosphor screen, biased to a high voltage, and imaged by a CCD camera. Plasma properties may also be diagnosed non-destructively by exciting and collective modes in the plasma (Tinkle et al., 1994).

2.2. Radial compression using a rotating electric field

One useful type of plasma manipulation that is likely to be crucial for accumulating large numbers of positrons is radial compression by the application of a rotating electric field to the plasma ("rotating wall"). This technique was first demonstrated for pure ion plasmas (Huang, 1997) and was later applied to electron and positron plasmas (Hollmann et al., 2000; Greaves, 2001). The rotating electric field is produced by applying suitable phased sine waves to an azimuthally segmented electrode surrounding the plasma as shown in Fig. 1. This excites rotating Trivelpiece-Gould (TG) waves which carry angular momentum. If the waves are damped, this momentum can be imparted to the particles, leading to plasma compression. If the plasma parameters are selected so that the excited TG mode is strongly damped, the resultant compression can be quite rapid (Greaves, 2001).

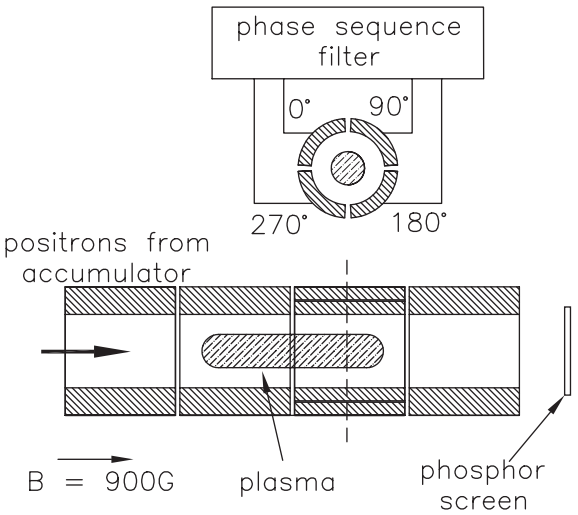

Fig. 1. Typical geometry for a Penning–Malmberg trap showing the confining electrodes with azimuthal segmentation for applying a rotating electric field.

3. Limits on the confinement of large numbers of positrons

3.1. The Brillouin limit

A collection of a single sign of charged particles of density n in a magnetic field of strength B, produces a radial space charge electric field E_r, the magnitude of which is proportional to the plasma density. This electric field causes the plasma to rotate about the direction, z, of the magnetic field. Up to a maximum density, the plasma can achieve an equilibrium configuration in which it rotates in the plane perpendicular to B as a rigid rotor. In this state, the outward-directed centrifugal and electric forces are balanced by the inward Lorentz force on the plasma. The limiting density n_B, commonly referred to as the Brillouin limit (Davidson, 1990), is given (in cgs units) by

$$n_B = \frac{B^2}{4\pi mc^2}, \tag{1}$$

where m is the mass of the charged particle and c is the speed of light. For positrons or electrons,

$$n_B = 5 \times 10^{12} \left(\frac{B}{1\,\mathrm{T}}\right)^2 B^2\,(\mathrm{cm}^{-3}). \tag{2}$$

In Eq. (2) and other "practical design" equations in this paper, we express magnetic fields in units of tesla, lengths in centimeters and electrical potentials in Volts. Unfortunately, as discussed below, we expect that devices designed to store large numbers of positrons will be limited by other factors than this Brillouin limit.

3.2. Space charge potential

The space charge of the plasma sets the minimum electrical potential required on the end electrodes to confine the plasma in the direction parallel to B. Practical considerations regarding the ability to impose large potential differences in vacuum make this an important consideration. For a long, uniform density cylindrical plasma inside cylindrical electrodes, the maximum space charge potential, ϕ_0, (which occurs at

radius $r = 0$) is given by

$$\phi_0 = \pi n e r_p^2 \left[1 + 2\ln\left(\frac{a_w}{r_p}\right)\right], \quad (3)$$

where r_p is the plasma radius, a_w is the inner radius of the cylindrical electrode confining the plasma, and the quantities are in cgs units. This condition can be written in terms of the number of positrons, N, and the plasma length, L_p,

$$\phi_0 = 1.4 \times 10^{-7} N \left(\frac{L_p}{1\,\mathrm{cm}}\right)^{-1} \left[1 + 2\ln\left(\frac{a_w}{r_p}\right)\right] \mathrm{(V)}. \quad (4)$$

Given that the objective is to store large numbers of positrons in a vacuum environment, Eq. (4) places an important practical constraint on the maximum number of particles per unit length that can be confined. In particular, the confining potential V_0 must be larger than ϕ_0. While not fully explored to date, the relatively large operating values of magnetic field may be an advantage here, as it will provide magnetic insulation. Using Eq. (4) and assuming a wall-to-plasma ratio, $\chi = a_w/r_p = 3$, the confinement of a positron line density $N/L_p = 2 \times 10^{10}\,\mathrm{cm}^{-1}$ requires a 10 kV potential on the confining electrodes. We note that for a spherically shaped plasma, the space charge potential per number of particles confined is larger than for a cylindrical plasma, and so the cylindrical geometry assumed here is favorable.

As a result of the constraint that Eq. (4) places on N/L_p, there has been proposed a multicell design in which multiple Penning–Malmberg traps are arranged in parallel and immersed in the same magnetic field (Greaves and Surko, 2002; Lynn, 2001). In the following, we build on this idea, taking into account the additional constraints imposed by outward plasma transport and the available amounts of plasma cooling.

3.3. Cross-field transport

The angular momentum of a single-component plasma in a strong magnetic field is proportional to $\sum_j r_j^2$, where r_j is the radial position of the jth particle. For a trap with no azimuthal asymmetries, there will be no torques on the plasma, and thus it is expected to reach a thermal equilibrium state. In this state, there would be no transport across the magnetic field, and so the plasma would have an infinite confinement time (O'Neil and Dubin, 1998). However, in practice there are observed to be practical limits on the confinement of these plasmas. In Fig. 2 are shown data by C.F. Driscoll and collaborators for the outward expansion rate, $\Gamma_0 = (1/n_0)(\mathrm{d}n_0/\mathrm{d}t)$, for electron plasmas measured in Penning–Malmberg traps (Hollmann et al., 2000; Hollmann, 1999). Here, n_0 is the central plasma density. In Fig. 2, the data are plotted as a function of the plasma "rigidity" $R = f_b/f_E$. This parameter R is the ratio of the

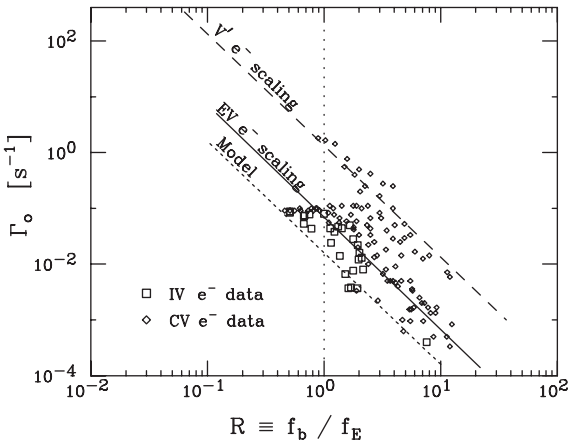

Fig. 2. The outward transport rate, Γ_0, from single-component electron plasmas is plotted as a function of the plasma rigidity, $R = f_b/f_E$ for various confinement devices. Shown are data from the IV and CV devices and scaling from the EV and V′ devices, studied by C.F. Driscoll and collaborators (Hollmann, 1999; Hollmann et al., 2000). The short-dashed line corresponds to Eq. (7), and parameterizes the smallest transport rates observed to date. Eq. (7) is used for the multicell trap design described here.

axial bounce frequency, $f_b = \overline{v_z}/2L_p$, to the $E \times B$ rotation frequency, f_E, of the plasma about the magnetic field direction where, for a plasma of uniform density n,

$$f_E = \frac{cne}{B}, \quad (5)$$

where $\overline{v_z}$ is the particle thermal velocity, and L_p is the length of the plasma and the quantities are in cgs units. In the assumed practical units

$$R = \frac{f_b}{f_E} = 1.5\left(\frac{B}{1\,\mathrm{T}}\right)\left(\frac{n}{10^{10}\,\mathrm{cm}^{-3}}\right)^{-1}\left(\frac{L_p}{1\,\mathrm{cm}}\right)^{-1}\left(\frac{T_p}{1\,\mathrm{eV}}\right)^{1/2}. \quad (6)$$

The unfavorable scaling of Γ_0 with plasma length and density are important constraints on the long-term confinement of high-density positron plasmas.

As illustrated in Fig. 2, the observed transport is found to vary from device to device and depends on factors such as whether the plasma is confined in one or several cylindrical electrodes. In general, the expansion rate can be characterized by the phenomenological relationship

$$\Gamma_0 = \frac{\Lambda}{R^2}, \quad (7)$$

where Λ is a device dependent constant that depends on the precision with which the trap and magnetic field coils are constructed. While the underlying origin of this transport is not presently understood, we assume for design purposes $\Lambda = 0.016\,\mathrm{s}^{-1}$, which is the (relatively small) transport rate, observed in recent, carefully constructed Penning–Malmberg traps. Eq. (7) with

$\Lambda = 0.016\,\mathrm{s}^{-1}$ is plotted as the short-dashed line in Fig. 2.

We note that there is some evidence that better confinement might be achieved using very cold plasmas in which the collision frequency $\nu_c \gg f_b$. (Malmberg et al., 1984). However, due to the relative lack of exploration off this regime, we will use Eq. (7) for the outward transport rate, Γ_0, in the multicell trap design described here, keeping in mind that further investigation of the regime of cold, highly collisional plasmas is warranted.

3.4. Plasma cooling

Cooling is required to counteract the plasma heating. This heating is due to the outward expansion of the plasma and the associated release of electrostatic potential energy and to the rotating wall electric fields. For electrons and positrons, two methods have been used, cooling with a buffer gas and cooling due to the emission of cyclotron radiation. For the situation considered here that requires long plasma confinement times (e.g., $>10^5$ s), annihilation and positronium formation losses make the use of buffer gas cooling impractical. In the case of cyclotron cooling, the cooling rate, $\Gamma_c = (1/T)(\mathrm{d}T/\mathrm{d}t)$, where T is the plasma temperature, is given by

$$\Gamma_c = \frac{1}{4}\left(\frac{B}{1\,\mathrm{T}}\right)^2 (\mathrm{s}^{-1}). \tag{8}$$

4. Design of a multicell trap

The space charge potential and the outward transport establish important constraints on the maximum achievable operating parameters of a positron trap. We assume that the outward expansion can be balanced by the application of rotating wall electric fields. However associated with the outward expansion of the plasma, there is plasma heating (i.e., a conversion of the electrostatic expansion energy into the thermal energy of the plasma particles). This heating will be present even when the mean plasma radius is kept constant using rotating wall compression. The heating rate, Γ_h, due to the outward transport is given by (Hollmann et al., 2000)

$$\Gamma_h = \frac{1}{T}\frac{\mathrm{d}T}{\mathrm{d}t} = \frac{e\phi_0}{\eta T}\Gamma_0, \tag{9}$$

where η is a constant of order unity. For the purposes of the model, we assume a constant density radial profile and find $\eta = [1 + 2\ln(a_w/r_p)]$. In order to obtain an estimate of the maximum density that can be obtained, we assume that this heating can be balanced by cyclotron cooling, with the cooling rate, Γ_c given by Eq. (8). We note that this assumption has never been tested experimentally and that there are some indications from recent experiments that a somewhat smaller cooling rate can achieve the desired effect, at least in some parameter regimes. However, we use this assumption as a basis for obtaining and order of magnitude of the density. Furthermore, we neglect any additional heating due to the "slip" in the rotating wall electric field, although in practice, this additional heating due to the rotating wall can be comparable to, or greater than Γ_h (Hollmann et al., 2000). If present, this heating must also be balanced by cyclotron cooling.

Noting these constraints, we equate Γ_h to Γ_c and find,

$$nL_p \leqslant 6\eta^{1/2}\left(\frac{B}{1\,\mathrm{T}}\right)^2\left(\frac{T}{1\,\mathrm{eV}}\right)\left(\frac{e\phi_0}{1\,\mathrm{eV}}\right)^{-1/2} (\mathrm{cm}^{-2}). \tag{10}$$

The inequality in Eq. 10 corresponds to the case in which additional heating is present due to the rotating wall electric fields. For design purposes, we will assume the trap operates with nL_p at its maximum value. Since nL_p is bounded from above and we want to achieve large positron densities for a compact positron trap, we choose to break up the plasma in the direction, z, of the magnetic field. Thus, we propose arranging multiple cells both perpendicular and parallel to z. A schematic of this geometry is shown in Fig. 3.

Eqs. (3) and (10) establish important constraints on n, L_p, and the total number of positrons, N_c, per plasma cell. For design purposes, we make a number of (in our view, relatively conservative) assumptions concerning the operating parameters of the trap. These assumptions are summarized in Table 1.

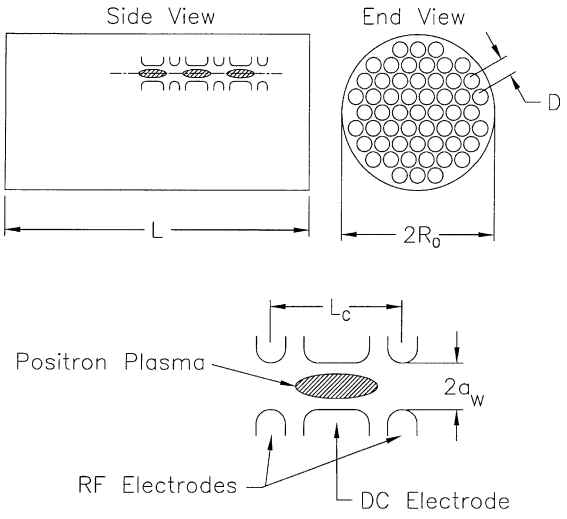

Fig. 3. Proposed geometry for a multicell trap for confining large numbers of positrons.

Table 1
Assumed operating parameters for a multicell positron trap

Parameter	Value
Space charge potential, ϕ_0	10 kV
Positron plasma temp., T	2 eV
Magnetic field, B	10 T
Plasma length, L_p	1 cm
Radius ratio, $\chi = a_w/r_p$	3
Overall length, L	1 m
Overall radius, R_0	0.25 m
Cell spacing (transverse), D	1.3 cm
Cell spacing (longitudinal), $L_p + \delta$	2 cm

Table 2
Calculated operating parameters of the multicell positron trap

Parameter	Value
Total number of positrons, N	1.5×10^{15}
Maximum electric field, E_m	20 kV/cm
Plasma density, n	2×10^{11} cm^{-3}
Plasma radius, r_p	0.18 cm
Plasma length, L_p	1 cm
Positrons per cell, N_c	2×10^{10}
Number of cells	70,000
Expansion rate, Γ_o	0.015 s^{-1}
Cooling rate, Γ_c	25 s^{-1}
Rigidity, R	1.0
Cooling/expansion heating power	0.01 W
$E \times B$ rotation freq., f_E	32 MHz
Rotating wall freq., f_{rw}	280 MHz
Plasma frequency, f_p	4.1 GHz
Cyclotron frequency, f_c	280 GHz

The choice of a particular operating value of the space charge potential ϕ_0 involves several considerations. We first describe a design assuming the maximum practical value for ϕ_0, and then discuss the characteristics of traps operating at smaller ϕ_0. Problems associated with arcing impose a practical upper limit on ϕ_0. We assume $\phi_0 = 10$ kV, which corresponds to maximum electric field values ~ 20 kV/cm. The maximum plasma temperature T will be bounded by the onset of positronium atom formation, which is the most rapid low-energy positron loss process for gas species typically present in UHV systems. We assume $T = 2$ eV. This corresponds to a positron lifetime $\geqslant 10^5$ s in a vacuum of 10^{-12} Torr, which is achievable using cryogenically cooled walls. We choose an easily achievable magnetic field of 10 T. In Table 1, the quantity δ is the extra space required for the end electrodes on each cell. These electrodes will be a minimum potential ϕ_0 above the central electrode of the cell. The choice of plasma length, L_p, is not critical. We choose $L_p = 1$ cm, but smaller values result in similar trap performance, so long as $L_p > r_p$.

Given the assumptions of Table 1, Eqs. (3) and (10) fix the maximum achievable plasma density, the minimum plasma radius, and maximum number of positrons per cell, N_c. We find: $n \leqslant 2 \times 10^{11}$ cm^{-3}, $r_p \geqslant 0.18$ cm, and $N_c = 2 \times 10^{10}$.

The goal is the confinement of the maximum number of positrons in a given volume, and so the cells should be arranged as closely packed as possible. We assume hexagonal close packing (HCP) in the plane perpendicular to B, in which case the total number of positrons will be

$$N = N_c \left(\frac{2\pi R_0^2}{\sqrt{3} D^2} \right) \left(\frac{L}{L_p + \delta} \right), \tag{11}$$

where R_0 and L are the length and radius of the trap (i.e., the entire collection of cells). The parameter D is the distance between the HCP cells in the direction transverse to B. In Eq. (11), the two factors in brackets are, respectively, the number of cells in a plane perpendicular to B and the number of cells in a line in the direction of B. With the values of parameters indicated in Table 1, Eq. (11) yields a maximum number of positrons, $N = 1.5 \times 10^{15}$. The operating parameters of the positron trap are summarized in Table 2. This design corresponds to an arrangement of Penning–Malmberg plasmas, 50 plasma cells in length and by approximately 40 cells in diameter. Using Eq. (9) and the assumed parameters, the heating due to expansion is given by $dQ/dt = N(dT/dt) = N(e\phi_0/\eta)\Gamma_0 \approx 0.01$ W.

In the operating regime described here, the rotating wall electric field must correspond to a low-order TG mode in the plasma that has a frequency f_{TG} such that f_{TG}/m_θ is not too far from the $E \times B$ rotation frequency, where m_θ is the azimuthal wave number of the mode (Hollmann et al., 2000). Neglecting the dependence of f_{TG} on T, the TG mode frequencies are given by

$$f_{TG} \cong f_p \frac{r_p k_z}{j[m_\theta, m_r]}, \tag{12}$$

where k_z is the wave number of the TG mode in the z direction, f_p is the plasma frequency, and $j[m_\theta, m_r]$ is the m_rth root of the m_θth Bessel function. We choose the $m_z = 1$, $m_r = 2$, $m_\theta = 2$, corresponding to a TG mode with frequency $f_{TG} = 280$ MHz. This represents a compromise between a low-order TG mode and one with frequency close to $(1/m_\theta)f_E$. We note that the required plasma compression rate is small compared to the maximum achieved in practice (Hollmann et al., 2000; Greaves, 2001). This is because the compression rate must only compensate the expansion rate, and the latter is bounded from above by the maximum available cooling power.

5. Discussion of the model

This model for a high-capacity trap assumes that the outward plasma transport can be balanced by rotating wall compression. It assumes that there will be an intrinsic heating associated with the expansion of the plasma (i.e., as expressed by Eq. (9)). This key feature of the model has not been verified in detail experimentally. The model also neglects heating associated with rotating wall compression. It assumes that the heating can be balanced by the cooling provided by cyclotron radiation. The design described above assumed a large space charge potential of 10 kV. We now discuss the possibility of operating at smaller values of ϕ_0. As expressed in Eq. (10), $nL_p \propto \phi^{-1/2}$. Since $N/L_p = \pi n r_p^2 \propto \phi_0$, the quantity $\xi = L_p/r_p^2 \propto \phi_0^{-3/2}$. Using Eq. (11), we find

$$N_{tot} \propto \phi_0 \xi \propto \phi_0^{-1/2}. \quad (13)$$

However, the increase in N with decreasing ϕ_0 comes at a price; namely the total number of cells scales as

$$N_{cells} \propto \phi_0^{-3/2}. \quad (14)$$

Thus more positrons can be confined at smaller values of ϕ_0, but this requires many more cells. The consequences of decreasing ϕ_0 are summarized in Table 3, assuming $L_p = 1$ cm. For fixed density, n, choosing a smaller value of L_p will yield a further decrease in the already small value of r_p.

As ϕ_0 is decreased, the plasma radius decreases and the number of cells increases. Both of these trends appear to introduce added complications. As the electrodes become smaller in diameter, alignment with respect to the magnetic field becomes more difficult. In particular, it is likely that alignment of the electrodes with the magnetic field must be done to $\leqslant 0.03 r_p$ over the 1 m length. As indicated in Table 3, this corresponds to a precision of 2 μm when working with a space charge of 100 V. All cells will require rotating wall electrodes and associated RF connections. At a minimum, a fraction of the cells will require extra plasma monitoring electrodes and electronics, and this number is likely to increase as the number of cells increases.

Another consideration is cyclotron cooling. At $B = 10$ T, the cyclotron radiation has a wavelength of 1 mm. Thus for values of r_p indicated in Table 3 at values of ϕ_0 below ≈ 1 kV, the cylindrical electrodes will begin to act as a wave-guide beyond cutoff and tend to inhibit cooling. Finally, at some point, the proximity of the plasmas to the inner wall of the electrodes is likely to lead to resistive damping of the plasma motion, which is known to destabilize the "negative energy" diocotron mode of the plasma (White et al., 1982). For these reasons, in the initial development of a multicell trap, a prudent first choice appears to be to work at a large value of ϕ_0 (e.g., the parameters summarized in Table 1).

Table 3
Number of positrons stored as a function of space charge potential, ϕ_0 for $L_p = 1$ cm

ϕ_o (V)	10	100	1×10^3	1×10^4
r_p (cm)	0.001	0.006	0.03	0.18
$2a_w$ (cm)	0.006	0.03	0.2	1.1
n (cm^{-3})	6×10^{12}	2×10^{12}	6×10^{11}	2×10^{11}
N_{tot}	5×10^{16}	1.5×10^{16}	5×10^{15}	1.5×10^{15}
N_{cells}	2×10^9	7×10^7	2×10^6	7×10^4

Note: The assumed electrode diameter is $6r_p$.

6. Trap development

There a number of attractive features of the approach outlined here to create a trap for large numbers of positrons. The operating parameters of the proposed design, i.e., $n \sim 2 \times 10^{11}$ cm^{-3}, $T = 2$ eV, $B = 10$ T and $r_p \sim 2$ mm, are not far from regimes of operation already studied using electron plasmas. Furthermore, the modular design tends to separate further development into manageable pieces. For example, the rotating wall compression and cyclotron cooling can be tested with a single plasma cell, independent of multicell operation. Similarly, aspects of the multicell design, such as manipulation of plasmas in in-line cells and the multiplexing, loading and control of cells in the transverse direction can also be tested separately.

There are also a number of important issues for experimental investigation. Optimization of the rotating wall compression must be done with plasmas in the assumed operating regime. Perhaps most important, it must be demonstrated that one can actually balance the outward transport (i.e., assumed to obey Eq. (7)) with rotating wall compression over a range of operating parameters, as assumed above. There are also a number of questions associated with the choice of rotating wall frequency. In particular, there will be tradeoffs to be considered concerning maximizing the coupling of the rotating wall electrodes to the plasma, maintaining stable operation, and minimizing plasma heating. Fortunately, all of these issues can be tested experimentally. To ensure efficient cyclotron cooling, it is likely that one will have to introduce in close proximity to each cell or group of cells, millimeter-wave cavities specifically designed to absorb efficiently at the cyclotron frequency.

Questions must also be addressed regarding multicell operation. Important issues include the simultaneous alignment of these many cells with respect to the magnetic field, and establishing efficient protocols for multicell loading and plasma storage and dumping. It is likely that in situ diagnostic capabilities will also be required, at least for a representative number of cells in the radial and longitudinal directions. A topic for later development will be determining the minimum number

of such control and diagnostic connections required for actual operation of a practical device. It is likely that many of these issues can be addressed with a smaller number of cells than the 70,000 called for in the full trap design.

If this design proves successful, there are also a number of ways in which the maximum number of stored positrons might be increased beyond the design goal of 10^{15} positrons discussed here. For example, one will undoubtedly try to optimize the operating value of space potential, ϕ_0. Also, if available, larger values of magnetic field would permit operation at larger plasma densities, thereby increasing N proportional to B^2.

7. Concluding remarks

In this paper, we have considered the design of a Penning–Malmberg trap capable of storing 10^{15} positrons. As mentioned above, one advantage of this design is that it utilizes single-component plasmas in a regime of parameter space not far from those already studied in the laboratory. More generally, even short of the 10^{15} design goal, further development of positron confinement devices such as the one described here has the potential to enable a wealth of new science and technology. A practical multicell trap might enable the development of portable positron (or antiproton) traps with a wide range of uses. Such traps are also likely to facilitate greatly research in areas that require large numbers of positrons, such as the creation and study of Bose-condensed positronium, study of electron–positron plasmas, and the creation and study of stable, neutral antimatter, such as antihydrogen.

Acknowledgements

We would like to acknowledge helpful conversations with F. Anderegg, C.F. Driscoll, and T.M. O'Neil. This work was supported by the Office of Naval Research.

References

Amoretti, M., Amster, C., Bonomi, G., et al., 2002. Nature 419, 456.

Davidson, R.C., 1990. Physics of Nonneutral Plasmas. Addison-Wesley, Redwood City, CA.

Gabrielse, G., Bowden, N.S., Oxley, P., et al., 2002. Phys. Rev. Lett. 89, 213401.

Greaves, R.G., Surko, C.M., 1997. Phys. Plasmas 4, 1528–1543.

Greaves, R.G., Surko, C.M., 2001. Phys. Plasmas 8, 1879.

Greaves, R.G., Surko, C.M., 2002. In: Anderegg, F., et al. (Ed.), Non-Neutral Plasma Physics, Vol. IV. American Institute of Physics, Melville, NY, pp. 10–23.

Hollmann, E.M., 1999. Unpublished Ph.D. Thesis, University of California, San Diego.

Hollmann, E.M., Anderegg, F., Driscoll, C.F., 2000. Phys. Plasmas 7, 2776–2789.

Huang, X.P., Anderegg, F., Hollmann, E.M., et al., 1997. Phys. Rev. Lett. 78, 875.

Lynn, K., 2001. Private communication.

Malmberg, J., et al., 1984. In: Sato, N. (Ed.), Proceedings of the 1984 Sendai Symposium on Plasma Nonlinear Electron Phenomena. Tohoku University, Sendai, Japan, pp. 31–36.

Mills Jr., A.P., 2002. Nuclear Instrum. Methods B 192, 107–116.

O'Neil, T.M., Dubin, D.H.E., 1998. Phys. Plasmas 5, 2163–2193.

Platzman, P.M., Mills, A.P., 1994. Phys. Rev. B 49, 454–458.

Schultz, P.J., Lynn, K.G., 1988. Rev. Mod. Phys. 60, 701–779.

Shertzer, J., Ackermann, J., Schmelcher, P., 1998. Phys. Rev. A 58, 1129–1138.

Surko, C.M., 2001. In: Surko, C.M., Gianturco, F.A. (Eds.), New Directions in Antimatter Chemistry and Physics. Kluwer Scientific Publishers, Dordrecht, The Netherlands, pp. 345–365.

Surko, C.M., Leventhal, M., Crane, W.S., et al., 1986. Rev. Sci. Instrum. 57, 1862–1867.

Tinkle, M.D., Greaves, R.G., Surko, C.M., Spencer, R.L., Mason, G.W., 1994. Phys. Rev. Lett. 72, 352–355.

White, W.D., Malmberg, J.H., Driscoll, C.F., 1982. Phys. Rev. Lett. 49, 1822.